



Original article

The actin binding protein destrin is associated with growth and perineural invasion of pancreatic cancer[☆]

Theresa Klose^{a,1}, Ivane Abiatari^{a,b,1}, Tamar Samkharadze^a, Tiago De Oliveira^a, Carsten Jäger^a, Merab Kiladze^c, Nataliya Valkovskaya^a, Helmut Friess^a, Christoph W. Michalski^a, Jörg Kleff^{a,*}

^a Department of Surgery, Technische Universität München, Munich, Germany

^b Institute of Medical Research, Ilia State University, Tbilisi, Georgia

^c Department of Surgery, Gudushauri National Medical Center, Tbilisi State University, Tbilisi, Georgia

ARTICLE INFO

Article history:

Received 12 February 2012

Received in revised form

31 May 2012

Accepted 31 May 2012

Keywords:

Pancreatic adenocarcinoma

Perineural invasion

Medical oncology

Pancreatic neoplasms

Destrin

Cofilin

Actin

Molecular biology

ABSTRACT

Background/Objectives: The small actin-binding protein destrin is one of the key regulators involved in remodeling of the actin cytoskeleton, a process crucial for cytokinesis, cell migration and polarized cell growth as well as for cancer cell migration and invasion.

Methods: A novel *ex vivo* nerve invasion model mirroring perineural cancer cell invasion as a key feature of pancreatic ductal adenocarcinoma has been previously established. Using this model, highly nerve-invasive clones of human pancreatic cancer cell lines have been obtained. Genome-wide transcriptional analyses of these cells revealed up-regulation of destrin in highly versus lowly nerve-invasive pancreatic cancer cells.

Results: Increased expression of destrin in these nerve-invasive cells was validated using quantitative RT-PCR and immunoblotting; concomitant changes in cell morphology were demonstrated using immunofluorescence analysis. Silencing of destrin by two specific siRNA oligonucleotides in Panc-1 pancreatic cancer cells decreased invasiveness and migration, and reduced proliferation of these cells.

Conclusions: Destrin is upregulated in nerve-invasive pancreatic cancer cells and its expression might be related to perineural invasiveness.

Copyright © 2012, IAP and EPC. Published by Elsevier India, a division of Reed Elsevier India Pvt. Ltd. All rights reserved.

1. Introduction

Pancreatic cancer is one of the most aggressive human tumors and the fourth leading cause of cancer related deaths in the Western world [1]. Absence of early symptoms leading to late diagnosis, the highly aggressive nature of the tumor with early metastasis to lymph nodes, the liver and other distant organs, as well as invasion to intra- and extrapancreatic nerve structures are key characteristics of this malignancy [2]. Perineural invasion (PNI) is a prominent and general feature of pancreatic cancer causing retropancreatic tumor extension and therefore precluding curative

resection in the majority of cases [3,4]. Consequently, perineural invasion has a strong impact on the local recurrence rate after tumor resection [5,6]. Despite its importance in pancreatic cancer, little is known about the mechanisms and genetic alterations in the tumor cells that influence invasion and migration into and along neural structures. To shed light on this subject, a novel PNI model has been established together with the consensus transcriptome signature of nerve invasive pancreatic tumor cells [7]. Of various differentially expressed genes, destrin (DSTN) displayed a significant up-regulation in cancer cells with a high capacity for nerve invasion.

DSTN belongs to the ADF/cofilin (AC) family which consists of three members in mammals (DSTN itself; cofilin-1 (CFL1) and the muscle-specific cofilin-2 (CFL2)). These proteins are abundant and essential in almost every eukaryotic cell type and belong to the so-called actin binding proteins [8–10]. They are involved in the modulation and precise regulation of the actin filament network. Actin filaments are irreplaceable for numerous cellular processes such as cell migration, cytokinesis, polarized cell growth and

[☆] This work was supported in part by grants from the Deutsche Krebshilfe 107750 (JK) and the Else-Kröner-Fresenius-Stiftung (JK and CWM).

* Corresponding author. Department of General Surgery, Technische Universität München, Ismaningerstrasse 22, 81675 Munich, Germany. Tel.: +49 89 4140 5098; fax: +49 89 4140 4870.

E-mail address: kleff@gmx.de (J. Kleff).

¹ These authors contributed equally to the study.

membrane trafficking [9,11]. These processes demand a rapid turnover of the actin filament network, termed actin dynamics. AC family proteins are key regulators of this turnover by enhancing it through de-polymerization and severing of the actin filaments. DSTN is the most potent turnover agent within this family [9,11,12]. Actin dynamics and their regulating proteins are not only essential for the normal development and function of the cell, but also play a crucial role in tumor cell metastasis, due to their influence on adhesion-dependent growth, cell motility and cell division [8,13,14]. Because actin cytoskeleton reorganization is important for cancer cell migration and invasion, we functionally analyzed DSTN, a pivotal regulator of the actin cytoskeleton and a potential novel player in perineural invasion of cancer cells.

2. Methods

2.1. Cell culture

8 pancreatic cancer cell lines: Panc-1, Colo357, T3M4, Aspc-1, BxPc-3, Capan-1, Mia paca-2 and SU8686 (kindly supplied by European Pancreatic Center, University of Heidelberg) were routinely grown in RPMI medium supplemented with 10% fetal calf serum (FCS), 100 units/ml penicillin, and 100 µg/ml streptomycin (complete medium). Cells were maintained at 37 °C in a humid chamber with 5% CO₂ and 95% air atmosphere [15].

2.2. Tissue sampling

PDAC tissue specimens (median age 62.5 years; range 41–78 years) and CP tissue specimens were obtained from patients who underwent pancreatic resections at the Departments of Surgery, University of Heidelberg, Germany and the Technische Universität München, Munich, Germany. Normal human pancreatic tissue samples were obtained from previously healthy individuals through an organ donor program. The Human Subjects Committees of the University of Heidelberg and the Technische Universität München approved all studies. Written informed consent was obtained from the patients.

2.3. Immunohistochemistry

Paraffin-embedded human pancreatic tissue sections (3-µm thick) were subjected to immunostaining as described previously [7]. Briefly, sections were deparaffinised in Roticlear (Carl Roth GmbH, Karlsruhe, Germany) and rehydrated in progressively decreasing concentrations of ethanol. Antigen retrieval was performed with citrate buffer (pH 6.0) in a microwave oven for 10 min. Endogenous peroxidase activity was quenched by incubating the slides with methanol containing 3% hydrogen peroxide. The sections were incubated at 4 °C overnight with the primary antibody, using a specific DSTN rabbit polyclonal antibody (cat. #: ab11072, Abcam, Cambridge, UK). The secondary anti-rabbit antibody (Dako Corp., Carpinteria, CA) was applied for 60 min at room temperature. Tissue sections were then subjected to 100 µl DAB-chromogen substrate mixture (Dako Corp.), followed by counterstaining with hematoxylin (Merck, Darmstadt, Germany). Slides were visualized using the Axioplan 2 imaging microscope (Carl Zeiss Lichtmikroskopie, Göttingen, Germany). As a negative control, rabbit IgG was used. Under these conditions, no specific immunostaining was detected.

2.4. Immunofluorescent cytochemistry

Cells were seeded in 8-well-chambers and allowed to grow overnight. Then, cells were washed with PBS, fixed with 1%

formaldehyde/PBS for 15 min at RT, permeabilized with 0.2% Triton X-100/PBS for 10 min, and subsequently blocked with 3% BSA/PBS for 30 min [7]. Slides were then incubated overnight with the primary rabbit polyclonal DSTN antibody at 4 °C. After that, slides were washed with PBS and incubated with fluorescent-labeled secondary antibody for 1 h at RT, together with Alexa Fluor® 488 phalloidin (Molecular probes, Inc. Eugene, OR) (for filamentous actin staining). Slides were mounted with DAPI (for nuclear counterstaining) and anti-fading medium (Gel/mount™, Abcam). Microscopic analysis was performed using the Axioplan 2 imaging microscope (Carl Zeiss).

2.5. Immunoblotting

Protein levels were assessed by immunoblotting as described previously [7] using the DSTN rabbit polyclonal antibody (Abcam) and CFL1 (D59) rabbit polyclonal antibody (Cell Signaling, Danvers, MA). Densitometry analysis of the blots was carried out using the ImageJ software (<http://rsbweb.nih.gov>).

2.6. Small interfering RNA transfection

For transient transfection, two different molecules of small interfering RNA (siRNA) for DSTN were used (Qiagen, Hilden, Germany); (DSTN siRNA#1 target sequence: TTGGTTGGAGATGTTGGTGA. DSTN siRNA#2 target sequence: TTAGGTGGATCCTTAATTGTA) (siRNA molecule sequences are validated by Qiagen). Cells were transfected using RNAi-Fect (Qiagen) as transfection reagent in 6-well plates [7]. Scrambled siRNA was used for control. Functional experiments were carried out after 96 h of transfection.

2.7. Proliferation assay

Anchorage-dependent cell growth was determined by the 3-(4,5-dimethylthiazol-2-yl)-2,5 diphenyltetrazolium bromide (MTT) colorimetric growth assay [7,16]. Briefly, 2000 cells per well were plated in 96-well plates and cultured for 2 days. Each day, cell growth was determined by adding MTT (50 µg/well) for 4 h. Mitochondrial MTT was solubilized with acidic isopropanol and absorbance was measured at 570 nm. The doubling time was calculated for the exponential growth phase. All experiments were performed in triplicates.

2.8. Real-time quantitative Polymerase Chain Reaction (QRT-PCR)

Total cellular RNA isolation and RNA extraction from normal and PDAC tissues was performed using the RNeasy Mini Kit according to the manufacturers' instructions. cDNA was synthesized from total RNA by reverse transcription using the QuantiTect Reverse transcription kit according to the manufacturers' recommendations. Real-Time PCR was performed with the LightCycler 480 DNA SYBR Green I Master kit. The primer sets were designed to amplify the common region of all transcript variants for DSTN (forward 5'-GGC CAG GGT CTC ACT GAG GGG-3', reverse 5'-CTC ACT GGC AGG TGC AGG GC-3') and CFL1 (forward 5'-TAT GAG ACC AAG GAG AGC AAG-3', reverse 5'-CTT GAC CTC CTC GTA GCA GTT-3'). The T_m value (58) of the primer was optimized by normal PCR which amplified a single band of DSTN and CFL1 at the predicted size. The calibration/standard curves were performed by a serial gradient dilution of cDNA. Intercept as well as Ct values of each single QRT-PCR were determined by the LightCycler 480 software. The target concentration was expressed as a ratio relative to the expression of the reference gene (β-actin) in the same sample and normalized to the calibrator sample. All experiments were repeated at least three times.

2.9. Matrigel invasion assay

Assays were done in 8 µm pore size BD Biocoat Matrigel Invasion Chambers (BD Biosciences) according to the manufacturers' instructions. 5 × 10⁴ cells/ml were added to the top chamber and incubated for 24 h. Cells adhering to the lower surface were fixed with 70% ethanol and stained with Mayer's hematoxylin. The whole membrane was scanned and the invading cells were counted. The assays were performed in duplicate and repeated three times.

2.10. Wound healing assays

An artificial "wound" was created using a 10 µl pipette tip on confluent cell monolayers in 6-well culture plates as described previously [7]. Quantification of "wound" closure was carried out by counting the number of cells in the "wound" area after 8 h. The cell number was expressed as the average per 3 optical fields.

2.11. Adhesion assay

5000 cells per well were plated in 96-well plates with complete medium. After 8 h of standard cell culture incubation, wells were washed 3 times with PBS and filled with 200 µl of medium per well containing MTT solution (50 µg/well) for 4 h. Following

solubilisation with acidic isopropanol, absorbance was measured at 570 nm. Values were normalized to control plates (incubated 5000 cells per well for 12 h and without the PBS washing step).

2.12. Statistical analysis

Results are expressed as mean ± standard error of the mean (SEM). For statistical comparisons, the non-paired student *t* test was used unless indicated otherwise. Survival analysis was carried out using the Kaplan–Meier method for estimation of event rates and the log-rank test for survival comparisons between patient groups. Significance was defined as *p* < 0.05.

3. Results

3.1. Destrin is upregulated in perineural invasive cells of pancreatic cancer

We have previously established an *ex-vivo* PNI model for pancreatic cancer and highly perineural invasive cancer cell clones (NP3) have been generated [7]. The *ex vivo* passaging of tumor cells through the nerves resulted in significant enrichment for several gene ontology processes including "cytoskeleton reorganization and cell motility" [7]. For further analysis here we selected DSTN

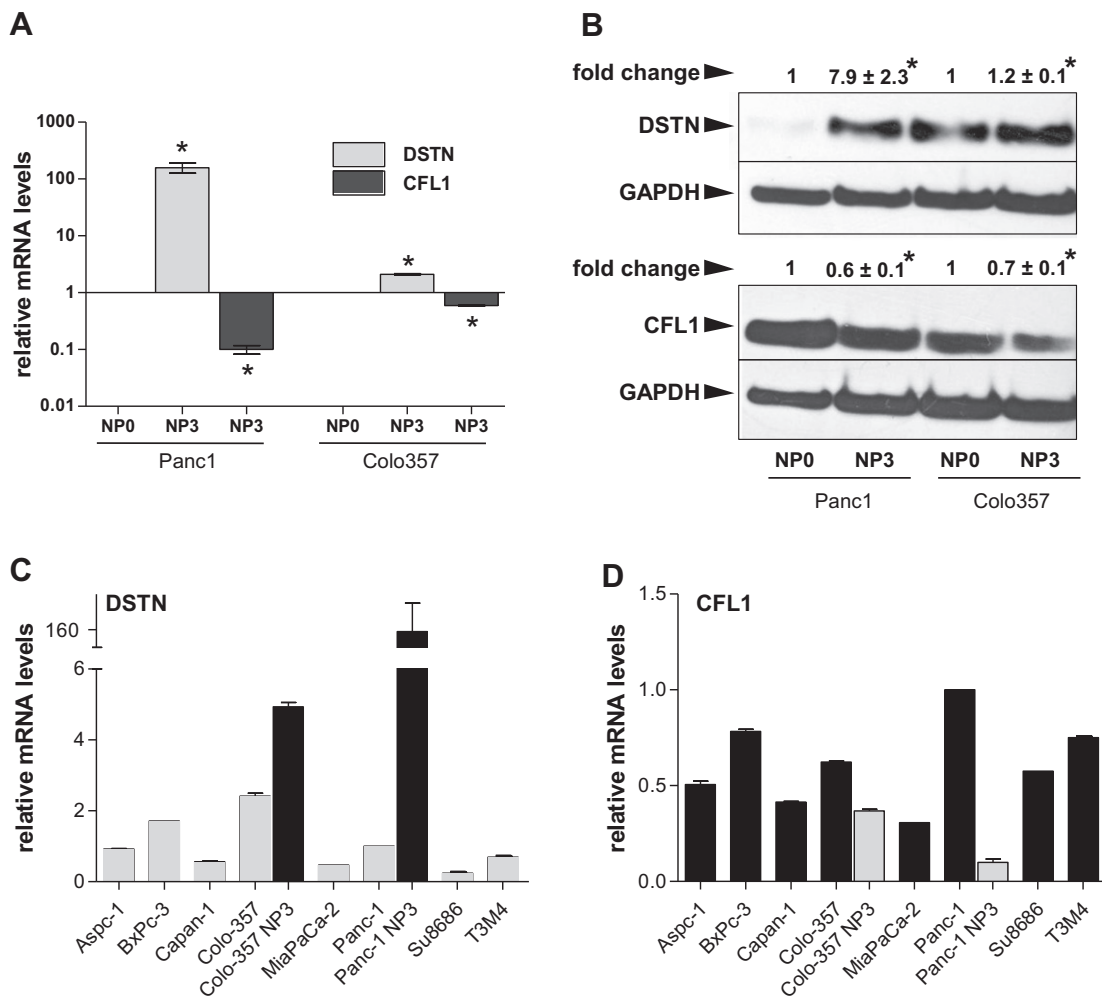


Fig. 1. Expression of DSTN and CFL1 mRNA and protein in lowly nerve invasive (NP0) and highly nerve invasive (NP3) pancreatic cancer cell clones using QRT-PCR (A) and immunoblot analysis (B) as described in the Materials and Methods section. Analysis of DSTN (C) CFL1 (D) mRNA expression in cultured pancreatic cancer cell lines (relative expression mRNA/β-actin). Data are presented as mean (±SEM) from three independent experiments. **p* < 0.05.

which was found as an important and differentially regulated (difference: 0.7 NPO-NP3 log₂) gene in this process. In this study, we investigated the expression of DSTN in perineural invasive pancreatic cancer cells at the mRNA and protein level. Quantitative RT-PCR revealed an increase of DSTN mRNA in NP3 clones compared to less nerve invasive (NPO) clones of both tested Panc-1 (158.5 ± 32.2 fold, $*p < 0.05$) and Colo357 (2.11 ± 0.05 fold, $*p < 0.05$) pancreatic cancer cell lines (Fig. 1A), confirming our previous micro-array results. DSTN up-regulation in nerve-invasive clones was also evident on the protein level comparing NPO versus NP3 clones (7.9 ± 2.3 fold for Panc-1 and 1.2 ± 0.1 fold for Colo357, $*p < 0.05$) (Fig. 1B). In order to analyze whether these changes were DSTN specific only, we also studied expression of the AC family gene CFL1 in these nerve invasive cells on the mRNA and protein level. Interestingly and in contrast to DSTN, mRNA expression of CFL1 in these nerve invasive clones was reduced in NP3 cells of Panc-1 (0.1 ± 0.01 fold, $*p < 0.05$) and Colo357 (0.6 ± 0.01 fold, $*p < 0.05$) cells compared to NPO clones (Fig. 1A). CFL1 was also downregulated on the protein level in NP3 clones compared NPO cells in Panc-1 (0.6 ± 0.1 fold, $*p < 0.05$) and Colo357 (0.7 ± 0.1 fold, $*p < 0.05$) cells (Fig. 1B). Analysis of different pancreatic cancer cells revealed endogenous expression of DSTN and CFL1 mRNA in all tested cancer cell lines ($n = 8$) (Fig. 1C,D).

Subsequently, we analyzed the expression of DSTN and CFL1 mRNA in normal pancreatic ($n = 10$), chronic pancreatitis (CP) ($n = 10$) and pancreatic cancer ($n = 20$) bulk tissues using quantitative RT-PCR. This analysis demonstrated decreased mRNA levels of DSTN and CFL1 in bulk pancreatic cancer tissues compared to

normal pancreas tissues (Fig. 2A,B). Interestingly, expression of DSTN mRNA above the median expression level correlated with shorter survival of the patients (number of analyzed samples: 58). However, this difference did not reach statistical significance ($p = 0.23$) (Fig. 2C). Furthermore, there was no correlation between DSTN mRNA expression and tumor grade as well (data not shown).

We next investigated the localization of this protein in pancreatic tissues. DSTN exhibited a cytoplasmic expression pattern in islets, acinar, ductal and nerve cells of normal pancreatic tissues (Fig. 3A,B). DSTN was also present in tubular complexes and hypertrophic nerves of pancreatic cancer tissues. Pancreatic cancer cells displayed strong DSTN expression and DSTN was also expressed in stromal cells of pancreatic cancer tissues (Fig. 3C–F). Moreover, DSTN was highly expressed in nerve invasive cancer cells of PDAC (Fig. 3G,H).

To further examine the functional relevance of DSTN in pancreatic cancer cells, we down-regulated endogenous expression levels of this protein using RNAi. The subsequent analyses were performed in NP3 Panc-1 pancreatic cancer cells, since in this cell line there was a clear expression difference of DSTN between NP3 and NPO pancreatic cancer cells (Fig. 1A,B). The efficacy of two siRNA molecules specific to DSTN mRNA in Panc-1-transfected cancer cells was confirmed on the protein level (Fig. 4A). The maximum reduction of DSTN expression to 0.2–0.3-fold compared to control-transfected cells was achieved 96 h after transfection. Expression of CFL1 was not significantly affected in these DSTN suppressed Panc-1 cells within 96 h of monitoring (Fig. 4A). Down-regulation of DSTN using specific siRNAs in Panc-1 NP3 pancreatic cancer cells resulted in

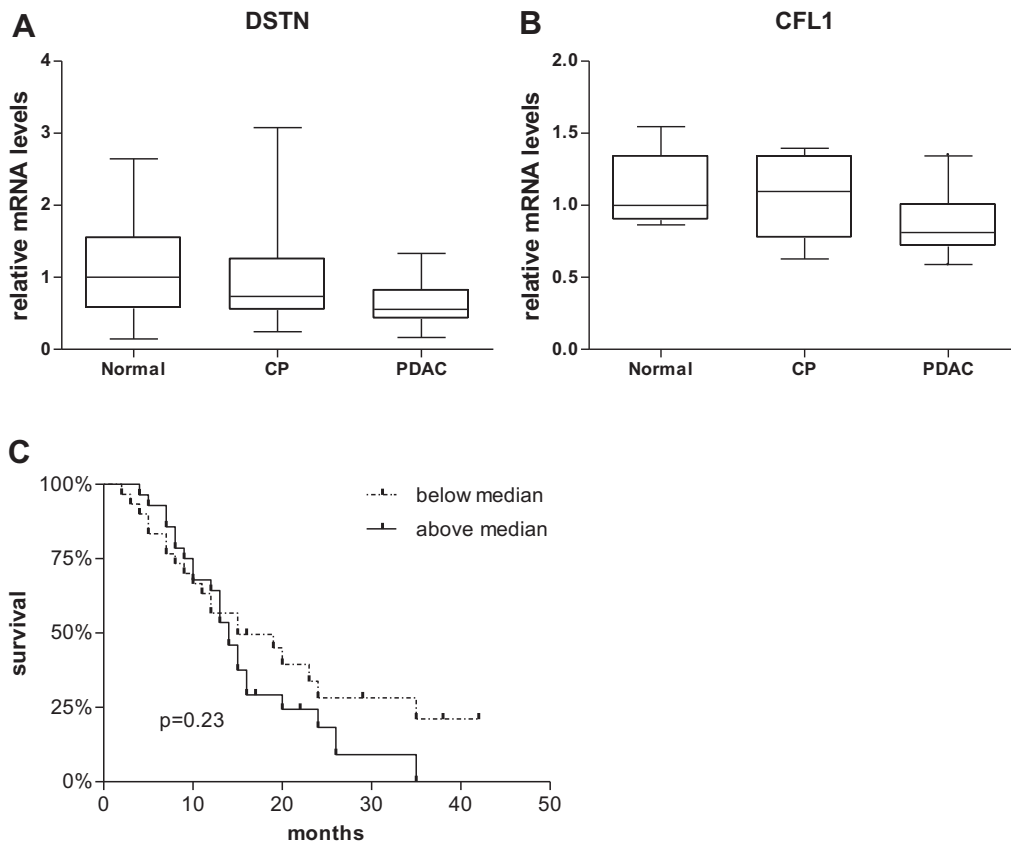


Fig. 2. Expression of DSTN (A) and CFL1 (B) mRNA in bulk normal pancreatic tissues ($n = 10$), chronic pancreatitis ($n = 10$) and pancreatic cancer ($n = 20$) tissues using QRT-PCR analysis, as described in the Materials and Methods section. Box and whisker plot with median expression level, interquartile range and 95% confidence interval. (C) The median value of DSTN expression was taken as cut-off to define groups with high (straight line) and low (dashed line) DSTN mRNA levels ($n = 58$). The survival of patients in these groups was compared using the Kaplan–Meier analysis and the log-rank test.

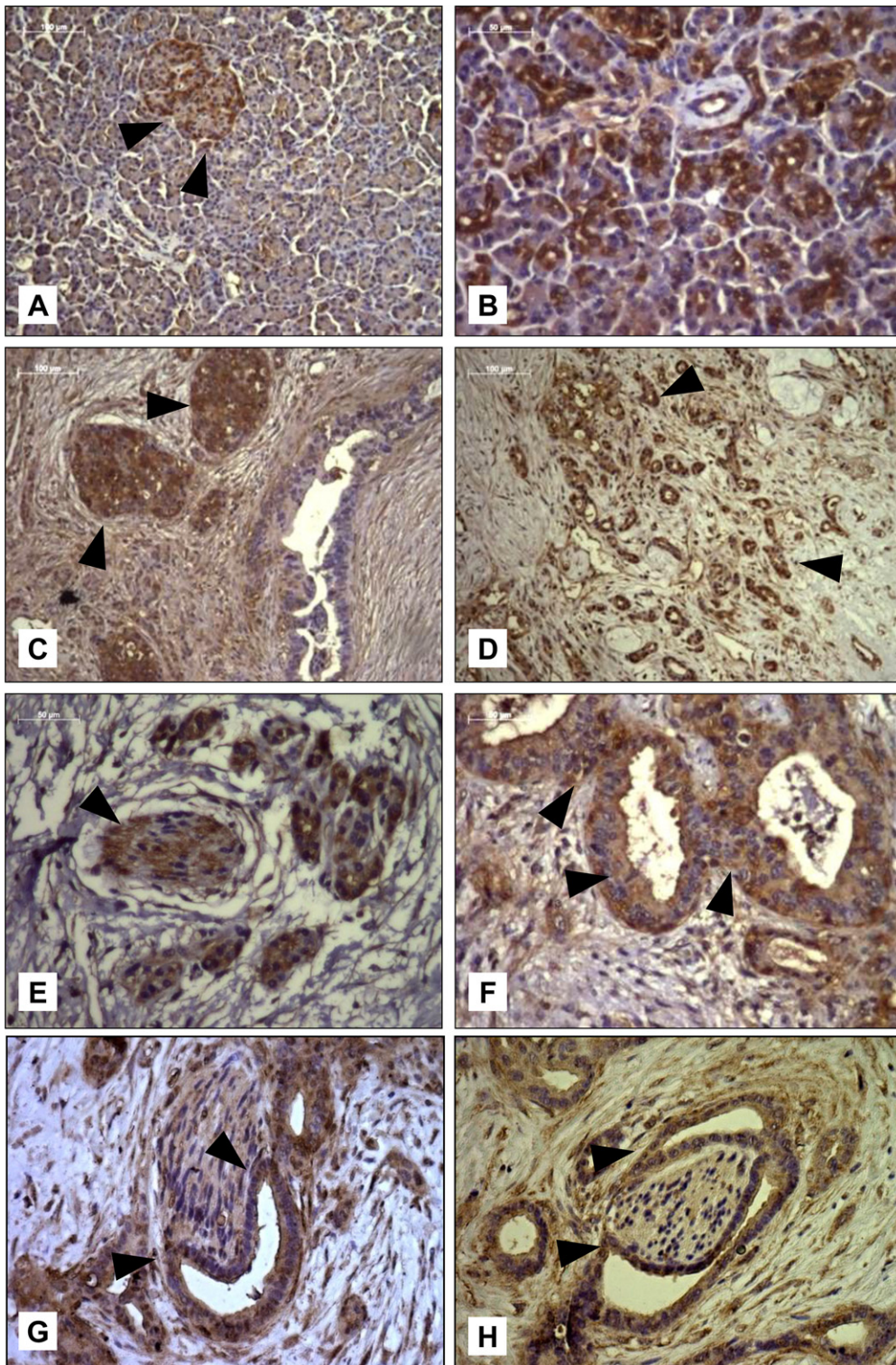


Fig. 3. Immunohistochemical analysis of normal pancreatic and ductal adenocarcinoma tissues using a specific DSTN antibody as described in the Materials and Methods section. Expression of DSTN in acini and islets of normal pancreas (A, B). Strong expression of DSTN in cancer cells, nerves and tubular complexes of pancreatic cancer tissues (C–H). Arrowheads indicate islets (A, C), tubular complexes (D), nerves (E), ductal adenocarcinoma cells (F) and perineural invasive cancer cells (G, H).

reduced proliferation (for siRNA#1: $126.7 \pm 7.9\%$ and for siRNA#2: $125.1 \pm 7.3\%$, at day 2) of these cells compared to control siRNA-transfected cells ($198.7 \pm 28.6\%$; $p < 0.05$; Fig. 4B).

Next, we tested the siRNA-transfected Panc-1 NP3 cells for potential changes in basal invasive properties. Proliferation controlled Matrigel invasion and wound healing assays revealed

decreased invasiveness (68% for siRNA#1 and 61% for siRNA#2) and reduced migratory activity (70% for siRNA#1 and 68% for siRNA#2) of DSTN-silenced cells compared to control cells ($p < 0.05$) (Fig. 4C). In contrast, adhesion assays did not reveal a significant difference in adhesion capacity between DSTN-silenced and control-transfected cells (Fig. 4C).

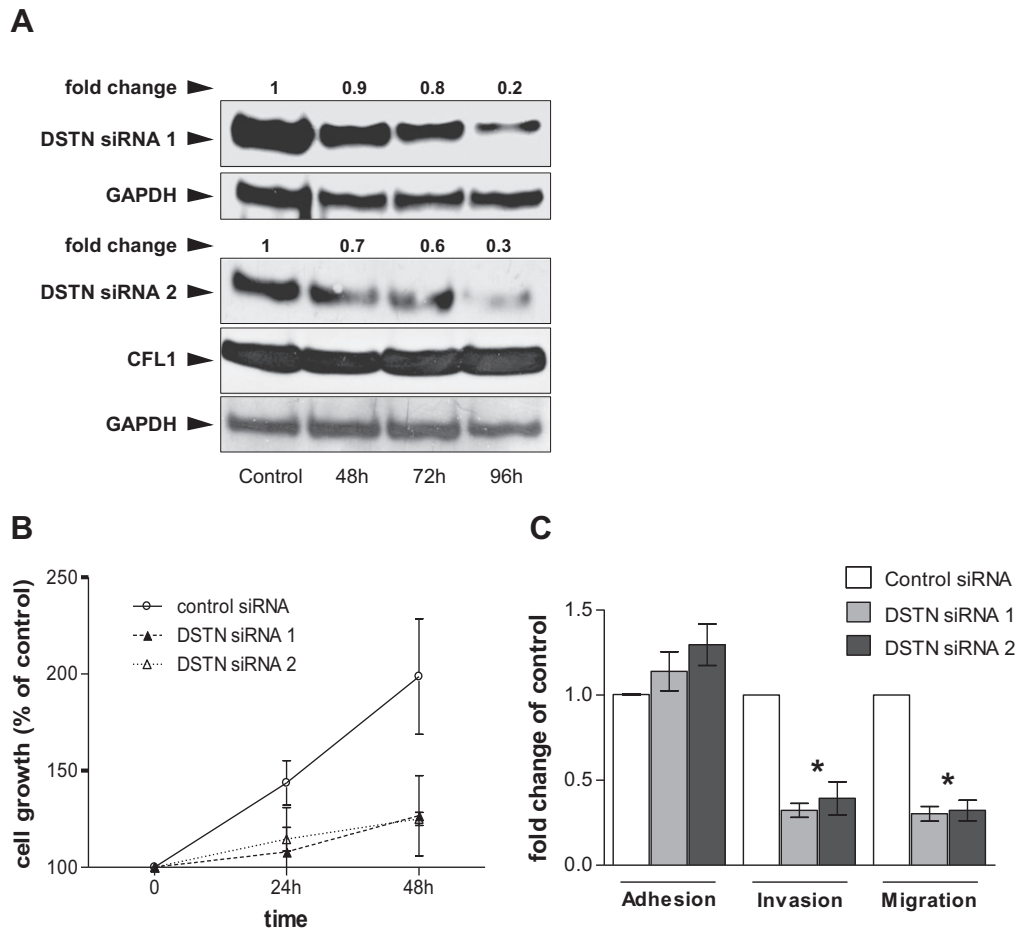


Fig. 4. (A) Immunoblot and densitometric analysis of DSTN and CFL1 expression in Panc-1 NP3 cells after siRNA transfections as described in the Materials and Methods section. (B) MTT assay analyzing the proliferation of DSTN silenced Panc-1 NP3 cells. (C) Adhesion, invasion and migration capacities of siRNA-transfected Panc-1 NP3 cells compared to control-transfected cells as described in the Materials and Methods section. Data are normalized to proliferation rate and presented as mean (\pm SEM) from three independent experiments. * $p < 0.05$.

For immunofluorescence analysis, a specific DSTN antibody as well as filamentous actin-specific phalloidin staining was used to determine differences in the morphology between NP0 and NP3 cells as well as in DSTN-silenced cells (Fig. 5A–D). Control cells demonstrated mainly nuclear and partly cytoplasmic expression pattern of DSTN (Fig. 5A,B), with the higher intensity in NP3 cells (Fig. 5B). Expression of DSTN was not detectable in DSTN-silenced cells (Fig. 5C,D). NP3 Panc-1 cells demonstrated solid organization of the actin cytoskeleton with dominant transverse stress fiber formation and well-defined adhesion junctions (Fig. 5B). In comparison, NP0 Panc-1 cells displayed poorly organized cortical actin localization with strikingly reduced cell–cell adhesion (Fig. 5A). Patterns of filamentous actin expression in NP3 cells were markedly changed after siRNA transfection of DSTN. These cells demonstrated reduced transversal stress fibers and increased cortical localization of actin (Fig. 5D). Interestingly, these changes in DSTN-silenced NP3 cells closely resembled the morphology of NP0 cells (Fig. 5A). Furthermore, down-regulation of DSTN expression induced a complete disorganization of the actin cytoskeleton in NP0 Panc-1 pancreatic cancer cells (Fig. 5C).

4. Discussion

Cancer cells show different modes of migration [17]. For example, single cancer cells are able to migrate in mesenchymal or amoeboid ways, and for both of these, reorganization of the actin

cytoskeleton is required [14]. It has been shown that manipulation of DSTN/CFL1 activity and its regulators, affects the formation of protrusions (e.g. lamellipodia) and cell migration since they are involved in invadopodia formation [18,19]. It is still unclear how the AC proteins exactly function in the mentioned processes and which circumstances lead to their different expression in cancer cells. It is not known whether DSTN and CFL1 share the same functions or either act independently or in a mutual manner in the actin dynamics of cell migration and invasion, however, the expression of DSTN and CFL1 is obviously differently regulated in perineural invasive pancreatic cancer cells. DSTN and CFL1 are highly similar to each other but they display differences in local expression and show quantitatively different effects on actin dynamics [12,20,21]. The AC pathway appears to have a central role in the generation of free actin filament ends resulting in actin filament remodeling by polymerization and de-polymerization. This process is essential during chemotaxis, cell migration and invasion of tumor cells. Therefore, a balance of stimulatory and inhibitory parts of the pathway is critical for these processes [22]. It is known that knockdown of either DSTN or CFL1 leads to defects in cell motility in mammalian (non-muscle) cells [9]. In *DSTN^{corn-1}* mice (spontaneous mutant mice which lack DSTN), the phenotype is mainly restricted to the cornea, where DSTN exists as the main AC family protein, suggesting a compensatory role of cofilins in other tissues [23]. It has been reported previously that DSTN/CFL1 isoforms are often co-expressed in the same cell types; nevertheless until

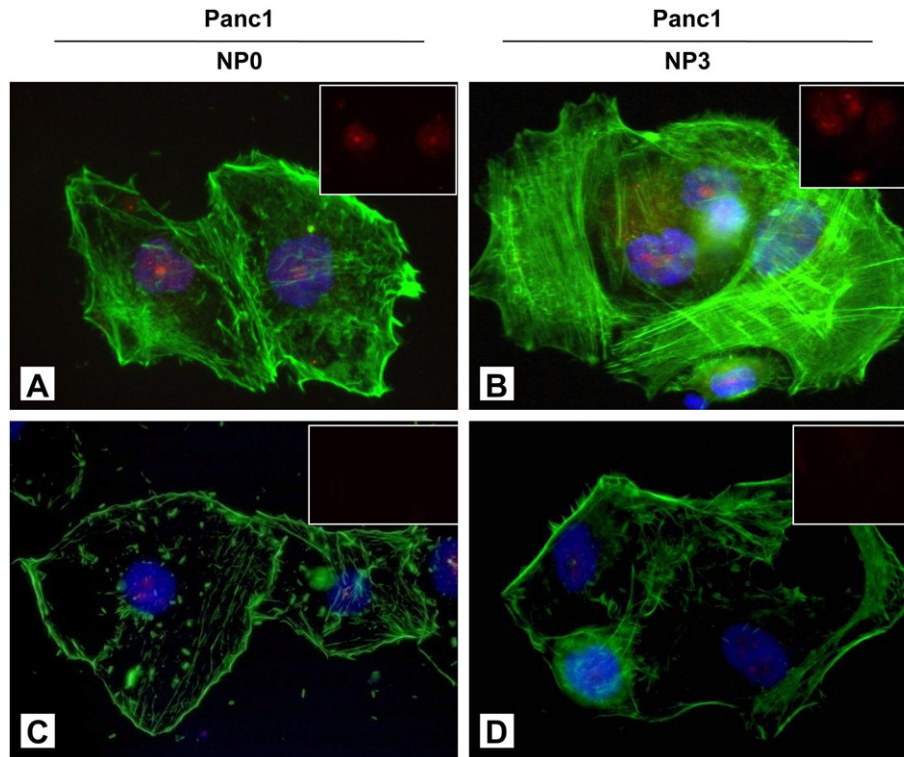


Fig. 5. Immunofluorescence of DSTN and actin organization in NP0 and NP3 Panc-1 pancreatic cancer cells. Analysis of DSTN siRNA- (C, D) and control- (A, B) transfected PNI clones of Panc-1 pancreatic cancer cells as described in the Materials and Methods section. Red: DSTN; green: F-actin; blue: nuclear counterstaining. (For interpretation of the references to colour in this figure legend, the reader is referred to the web version of this article.)

now, the exact reasons for this co-expression have not been elucidated [18].

Our recently published PNI genome-wide transcriptional analyses [7] revealed expression changes of DSTN, which was verified by QRT-PCR and immunoblotting experiments. Additionally, in the present study, DSTN-depleted highly nerve invasive cells displayed a significantly altered phenotype as shown by immunofluorescence staining. These results point towards a strong influence of DSTN expression on the actin cytoskeleton organization of these cells. Migration and invasion assays with DSTN knock out NP3 cells also showed significant functional changes in these cells. We have surprisingly observed that the invasive phenotype of PNI cells displayed a more organized actin cytoskeleton rather than the expected disorganized morphology. The reasons for this discrepancy are currently not known and have to be further investigated. It could be speculated that DSTN has stronger actin filament de-polymerization activity than CFL1 [12,20]. Interestingly, DSTN is up-regulated in platinum-resistant ovarian cancer cells [24]. CFL1 appears to be over-expressed in human chemoresistant pancreatic adenocarcinoma [25]. Whether DSTN is involved in chemoresistance of pancreatic cancer is currently unknown and might be an interesting topic to investigate. Further studies have to be carried out to better understand this potential interaction.

Up-regulation of DSTN has also been observed in other tumor diseases, e.g. in primary anaplastic thyroid cancer and its derived cell lines as well as in malignant lung epithelial cells [26,27]. Furthermore, DSTN is expressed in all examined colon cancer cell lines so far. In the Isreco1 colon carcinoma cell line, DSTN and CFL1 are expressed at a comparatively high level, but interestingly only DSTN appears to be required for cell migration and cell invasion [28]. In rat ascites hepatoma cells, simultaneous knockdown of DSTN and CFL1 using specific siRNA decreased the motility and transcellular migration of these cells in two-dimensional culture.

Knockdown of LIMK1, a kinase which inactivates the AC family of proteins through phosphorylation at Ser-3 [29,30], suppressed fibronectin-mediated cell attachment and focal adhesion formation [31]. In our approach, silencing of DSTN resulted in only slightly increased adhesion. Possibly, down-regulation of DSTN alone is not sufficient to increase adhesion in invasive pancreatic cancer cells and depends on additional factors. It is unknown whether down-regulation of CFL1 expression in PNI pancreatic cancer cells is directly induced or linked to the up-regulation of DSTN. However, our results indicate an involvement of the AC pathway in this phenomenon. DSTN has to be considered as one effector molecule in the actin dynamics - a complex process with precise spatial and temporal regulation. Therefore, besides DSTN, the AC family of proteins and their direct or upstream regulators, such as: LIMK1/2, SSH1-3 and rho family small GTPases, are involved in migration and invasion of cancer cells [7,14,18,22,31,32]. Targeting an effector at the end of complex signaling pathways such as DSTN may therefore be of particular interest for developing successful therapeutic concepts.

References

- [1] Siegel R, Naishadham D, Jemal A. Cancer statistics. *CA: A Cancer Journal Clinicians* 2012;62:10–29.
- [2] Kleeff J, Michalski C, Friess H, Buchler MW. Pancreatic cancer: from bench to 5-year survival. *Pancreas* 2006;33:111–8.
- [3] Hirai I, Kimura W, Ozawa K, Kudo S, Suto K, Kuzu H, et al. Perineural invasion in pancreatic cancer. *Pancreas* 2002;24:15–25.
- [4] Yi SQ, Miwa K, Ohta T, Kayahara M, Kitagawa H, Tanaka A, et al. Innervation of the pancreas from the perspective of perineural invasion of pancreatic cancer. *Pancreas* 2003;27:225–9.
- [5] Beger HG, Rau B, Gansauge F, Poch B, Link KH. Treatment of pancreatic cancer: challenge of the facts. *World J Surg* 2003;27:1075–84.
- [6] Liu B, Lu KY. Neural invasion in pancreatic carcinoma. *Hepatobiliary Pancreat Dis Int* 2002;1:469–76.

- [7] Abiatari I, DeOliveira T, Kerkadze V, Schwager C, Esposito I, Giese NA, et al. Consensus transcriptome signature of perineural invasion in pancreatic carcinoma. *Mol Cancer Ther* 2009;8:1494–504.
- [8] Chen H, Bernstein BW, Bamburg JR. Regulating actin-filament dynamics in vivo. *Trends Biochem Sci* 2000;25:19–23.
- [9] Hotulainen P, Paunola E, Vartiainen MK, Lappalainen P. Actin-depolymerizing factor and cofilin-1 play overlapping roles in promoting rapid f-actin depolymerization in mammalian nonmuscle cells. *Mol Biol Cell* 2005;16:649–64.
- [10] Maciver SK, Hussey PJ. The adf/cofilin family: actin-remodeling proteins. *Genome Biol* 2002;3: reviews3007.
- [11] Bamburg JR, McGough A, Ono S. Putting a new twist on actin: adf/cofilins modulate actin dynamics. *Trends Cell Biol* 1999;9:364–70.
- [12] Yeoh S, Pope B, Mannherz HG, Weeds A. Determining the differences in actin binding by human adf and cofilin. *J Mol Biol* 2002;315:911–25.
- [13] Bamburg JR, Wiggan OP. Adf/cofilin and actin dynamics in disease. *Trends Cell Biol* 2002;12:598–605.
- [14] Yamazaki D, Kurisu S, Takenawa T. Regulation of cancer cell motility through actin reorganization. *Cancer Sci* 2005;96:379–86.
- [15] Li J, Kleeff J, Abiatari I, Kaye H, Giese NA, Felix K, et al. Enhanced levels of hulf-1 interfere with heparin-binding growth factor signaling in pancreatic cancer. *Mol Cancer* 2005;4:14.
- [16] Herner A, Sauliunaite D, Michalski CW, Erkan M, De Oliveira T, Abiatari I, et al. Glutamate increases pancreatic cancer cell invasion and migration via ampa receptor activation and kras-mapk signaling. *Int J Cancer*; 129: 2349–2359.
- [17] Friedl P, Wolf K. Tumour-cell invasion and migration: diversity and escape mechanisms. *Nat Rev Cancer* 2003;3:362–74.
- [18] Van Troys M, Huyck L, Leyman S, Dhaese S, Vandekerckhove J, Ampe C. Ins and outs of adf/cofilin activity and regulation. *Eur J Cell Biol* 2008;87: 649–67.
- [19] Yamaguchi H, Lorenz M, Kempiak S, Sarmiento C, Coniglio S, Symons M, et al. Molecular mechanisms of invadopodium formation: the role of the n-wasp-arp2/3 complex pathway and cofilin. *J Cell Biol* 2005;168: 441–52.
- [20] Vartiainen MK, Mustonen T, Mattila PK, Ojala PJ, Thesleff I, Partanen J, et al. The three mouse actin-depolymerizing factor/cofilins evolved to fulfill cell-type-specific requirements for actin dynamics. *Mol Biol Cell* 2002;13:183–94.
- [21] Moriyama K, Nishida E, Yonezawa N, Sakai H, Matsumoto S, Iida K, et al. Destrin, a mammalian actin-depolymerizing protein, is closely related to cofilin. Cloning and expression of porcine brain destrin cDNA. *J Biol Chem* 1990;265:5768–73.
- [22] Wang W, Eddy R, Condeelis J. The cofilin pathway in breast cancer invasion and metastasis. *Nat Rev Cancer* 2007;7:429–40.
- [23] Verdoni AM, Aoyama N, Ikeda A, Ikeda S. Effect of destrin mutations on the gene expression profile in vivo. *Physiol Genomics* 2008;34:9–21.
- [24] Yan XD, Pan LY, Yuan Y, Lang JH, Mao N. Identification of platinum-resistance associated proteins through proteomic analysis of human ovarian cancer cells and their platinum-resistant sublines. *J Proteome Res* 2007;6:772–80.
- [25] Sinha P, Hutter G, Kottgen E, Dietel M, Schandendorf D, Lage H. Increased expression of epidermal fatty acid binding protein, cofilin, and 14-3-3-sigma (stratifin) detected by two-dimensional gel electrophoresis, mass spectrometry and microsequencing of drug-resistant human adenocarcinoma of the pancreas. *Electrophoresis* 1999;20:2952–60.
- [26] Chang JW, Jeon HB, Lee JH, Yoo JS, Chun JS, Kim JH, et al. Augmented expression of peroxiredoxin i in lung cancer. *Biochem Biophys Res Commun* 2001;289:507–12.
- [27] Onda M, Emi M, Yoshida A, Miyamoto S, Akaishi J, Asaka S, et al. Comprehensive gene expression profiling of anaplastic thyroid cancers with cDNA microarray of 25 344 genes. *Endocr Relat Cancer* 2004;11:843–54.
- [28] Estornes Y, Gay F, Gevrey JC, Navoizat S, Nejari M, Scoazec JY, et al. Differential involvement of destrin and cofilin-1 in the control of invasive properties of isreco1 human colon cancer cells. *Int J Cancer* 2007;121: 2162–71.
- [29] Arber S, Barbayannis FA, Hanser H, Schneider C, Stanyon CA, Bernard O, et al. Regulation of actin dynamics through phosphorylation of cofilin by lim-kinase. *Nature* 1998;393:805–9.
- [30] Yang N, Higuchi O, Ohashi K, Nagata K, Wada A, Kangawa K, et al. Cofilin phosphorylation by lim-kinase 1 and its role in rac-mediated actin reorganization. *Nature* 1998;393:809–12.
- [31] Horita Y, Ohashi K, Mukai M, Inoue M, Mizuno K. Suppression of the invasive capacity of rat ascites hepatoma cells by knockdown of slingshot or lim kinase. *J Biol Chem* 2008;283:6013–21.
- [32] Bernard O. Lim kinases, regulators of actin dynamics. *Int J Biochem Cell Biol* 2007;39:1071–6.